Journal Pre-proof

Green core clinopyroxenes from Martin Vaz archipelago Plio-Pleistocenic alkaline rocks, south atlantic ocean, Brazil: A magma mixing and polybaric crystallization record

André Leite de Oliveira, Anderson Costa dos Santos, Camila Cardoso Nogueira, Thaís Mothé Maia, Mauro César Geraldes

PII: S0895-9811(20)30494-6

DOI: https://doi.org/10.1016/j.jsames.2020.102951

Reference: SAMES 102951

To appear in: *Journal of South American Earth Sciences*

Received Date: 15 May 2020

Revised Date: 7 October 2020

Accepted Date: 7 October 2020

Please cite this article as: Leite de Oliveira, André., Costa dos Santos, A., Nogueira, C.C., Maia, Thaí.Mothé., Geraldes, Mauro.Cé., Green core clinopyroxenes from Martin Vaz archipelago Plio-Pleistocenic alkaline rocks, south atlantic ocean, Brazil: A magma mixing and polybaric crystallization record, *Journal of South American Earth Sciences* (2020), doi: https://doi.org/10.1016/j.jsames.2020.102951.

Journal of South American Earth Science

Rio de Janeiro, august 21st, 2020

Author Statement

Dear Editor-in-chief,

Please find bellow the authorships contribution related to the manuscript entitled “Green-core clinopyroxenes from Martin Vaz Archipelago Plio-Pleistocenic alkaline rocks, South Atlantic Ocean, Brazil: a magma mixing and polybaric crystallization record”, SAMES NUMBER: SAMES-D-20-00295.

André Leite de Oliveira: conceptualization, development, validation, investigation, original draft, formal analyzes and visualization. Anderson C. dos Santos: conceptualization, methodology, investigation, resources, data curation, supervison and project administration. Camila C. Nogueira: investigation, supervision, review and editing. Thaís M. Maia: formal analysis. Mauro C. Geraldes: resources, project administration and funding acquisition.

Green core clinopyroxenes from Martin Vaz Archipelago Plio-Pleistocenic alkaline rocks, South Atlantic Ocean, Brazil: a magma mixing and polybaric crystallization record

[1a]André Leite de Oliveira; [1b]Anderson Costa dos Santos; [1c]Camila Cardoso Nogueira; [1d]Thaís Mothé Maia; [1e]Mauro César Geraldes

[1]Universidade do Estado do Rio de Janeiro (UERJ), Faculdade de Geologia, Departamento de Mineralogia e Petrologia Ígnea (DMPI). São Francisco Xavier Street, 524 - 4033A, Rio de Janeiro (RJ), Brazil, [1b*] Tektos and GeoAtlântico groups, Rio de Janeiro State University/Geobiotec, Geosciences Department, Aveiro University, 3810-193 Aveiro, Portugal.

[1a] Corresponding author: andre.leite.quatis@gmail.com
ORCID: [1a]https://orcid.org/0000-0001-6340-5679; [1b]https://orcid.org/0000-0003-2526-8620; [1c]https://orcid.org/0000-0002-5201-2367; [1d]https://orcid.org/0000-0002-5956-6362; [1e]https://orcid.org/0000-0003-2914-2814

Abstract

The Martin Vaz Archipelago is located at the parallel 20°S, 1200 km away from the Brazilian coastline and is composed of Plio-Pleistocenic alkaline rocks that represent the last volcanic event of the Vitória-Trindade Ridge. The Archipelago is divided into three main units: Pico das Gaivotas Unit (i) is made up of nosean-phonolite and phono-tephrite domes and tephri-phonolite dykes with clinopyroxene, nosean and potassic feldspar phenocrysts, and scarce kaersutite anhedral phenocrysts; the Bandeira Unit (ii), in turn, comprises melanephelinitic and basanitic lava flows with olivine and clinopyroxene (diopside) phenocrysts; and lastly, the Basal Unit (iii) is composed of pyroclastic deposits with tuffs, lapilli-tuffs and lapillite. The clinopyroxene phenocrysts from Pico das Gaivotas and Bandeira Units have anhedral green cores with sieved and poikilitic textures and show reaction rims composed of opaque minerals, indicating disequilibrium and compositional changes in the liquid. This study provides mineral chemistry data indicating that clinopyroxene rims are more primitive (Mg# 57.46 – 84.12) and enriched in Al-Ti-Fe^{3+}-Ca compared to the Fe-rich green-cores, probably related with a more primitive Ca-rich magma input in the magmatic chamber after the green-core crystallization from a different liquid. Olivine crystals from Bandeira Unit show resorption features and no compositional affinity with the analyzed liquid, indicating that these crystals have a xenocrystic origin from mantle peridotitic source. Clinopyroxene geothermobarometry data suggest different pressure and temperature

conditions for cores and rims during crystallization, reflecting a polybaric evolutionary history. Pico das Gaivotas Unit clinopyroxene phenocrysts suggest a particularly higher-pressure environment, and a complex evolutionary history.

Keywords: Martin Vaz Archipelago, Magma chamber replenishment, Magma Mixing, Metasomatism**,** Green core clinopyroxenes**.**

1 Introduction

Green-core clinopyroxenes genesis has been interpreted as a result of magma mixing process (Dobosi & Fodor, 1992; Neumann *et al*., 1999), polybaric crystallization (Duda & Schmincke, 1985; Fodor *et al*., 1995; Santos, 2016), increased oxygen or water fugacity (Holm, 1982; Aurisicchio *et al.*, 1988) or a xenocrystic origin related to the parental peridotites magmas (Jung *et al*., 2006). These variable origins should be analysed by observing the relationship between clinopyroxenes and olivines with high Mg# liquid content (Barton & Van Bergen, 1981; Fodor *et al*., 1995; Xu *et al.*, 2003).
Alumina contents reveal important information regarding to the depth of crystallization and relationship between crystalline phases from mantle-derived melts. According to Dobosi and Fodor (1992), high Al content expressed by Al^{VI}/Al^{IV} and Ti/Al ratios indicates crystallization in high pressure conditions. Le Bas (1962) suggests that the alumina content in clinopyroxenes increases with the alkalinity of the magma together with Ti and Fe (Barberi *et al*., 1971). Related to that, under conditions of high pressure and solid-liquid equilibrium, Al atoms enter in the octahedral sites in the forming compatible mineral phase.

Martin Vaz Archipelago is located *ca.* 1200 km off Brazilian coastline in the parallel ~20° S and it represents the last volcanic expression of the Vitória-Trindade Ridge during the Plio-Pleistocene (VTR - Figure 1). This archipelago is composed of a basal unit containing pyroclastic deposits covered by nephelinitic lava flows, that sometimes shows interbedding. These lava flows (Bandeira Unit - 0.49 ± 0.08 – 0.63 ± 0.12 Ma; Santos, 2016) are composed of two faciological units: (1) olivine basanite and (2) melanephelinite. Bandeira Unit is cut by Pico das Gaivotas Unit (0.64 ± 0.08 Ma - Santos, 2016) composed of tephri-phonolitic and nosean-phonolite domes and radial phono-tephritic dykes.
The present work details petrographic features, mineral chemistry and geothermobarometry data of green core clinopyroxenes from Plio-Pleistocenic

nephelinitic and phonolitic rocks from Martin Vaz main Island to access information related to evolutionary constraints and P-T crystallization conditions for the youngest peralkaline magmatism in the Brazilian territory.

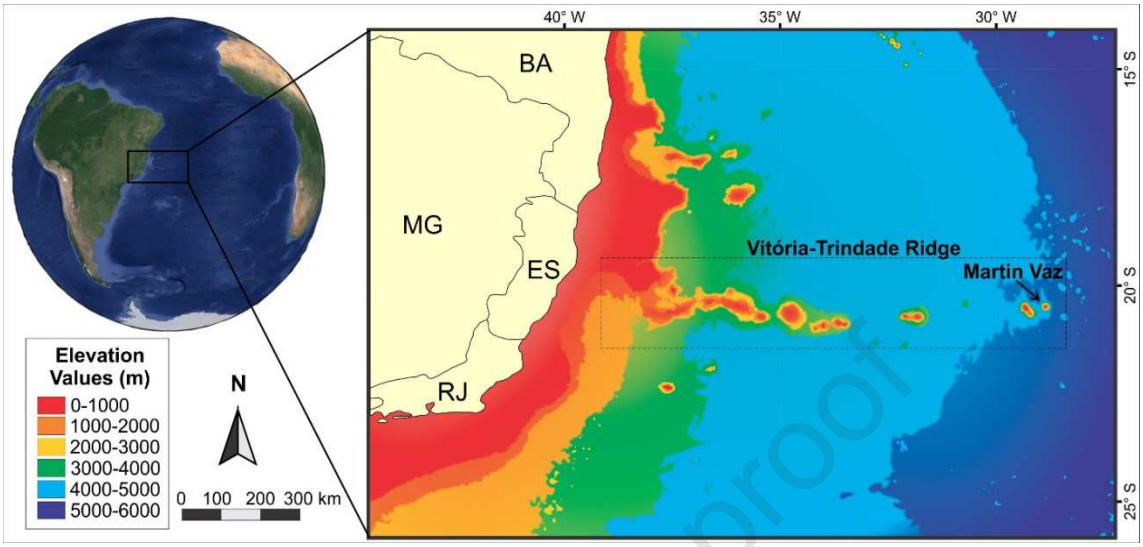

Figure 1: Localization of the Martin Vaz Archipelago, in the context of Vitória-Trindade Ridge at the parallel 20º south, 1200 Km away from the Brazilian Coastline (data ETOPO-NOAA, Amante & Eakins, 2009; Google Earth Pro).

2 Brief considerations on Martin Vaz Island geology and petrology

There are few publications about Martin Vaz geology, since the archipelago is difficult to be accessed. The first detailed scale map (1:5000) was made by Santos *et al.* (2015, modified in Figure 5), which separated the lithotypes into four units: (i) the Basal one, composed of pyroclastic deposits (tuffs, lapilli-tuffs and lapillite), (ii) nephelinitic flows (Bandeira Unit) that occurs interbedded with the pyroclastic deposit and it has a petrographic distinction into two facies: olivine basanite and melanephelinite, and (iii) phono-tephrite/nosean-phonolite domes named as Pico das Gaivotas Unit with associated tephri-phonolite dykes, predominantly radial on the main island, also observed on the North and South islands and Pico das Agulhas islet (Santos *et al.*, 2015).

Scorza (1964) first described the alkaline rocks of Martin Vaz Island as ankaratrite and haüynite. Cordani *et al.* (1970) obtained the first K-Ar ages from the same blocks described by Scorza (1964), with one absolute age of *ca*. 60 Ma for the ankaratrite, but considered questionable due to the tectonic context, and yielded a second age, younger than *ca*. 0.73 Ma for the hayünite. Santos & Marques (2007) acquired isotopic dating using U-Th-Ra and Th-Ra-Th methods and yielded ages of about 300 Ka. Santos (2013;

2016) and Santos *et al.* (2015) obtained $^{40}Ar/^{39}Ar$ ages between 0.49 ± 0.08 Ma and 0.63 ± 0.12 Ma for the Bandeira Units, and 0.64 ± 0.08 Ma for Pico das Gaivotas Unit.

Marques *et al.* (1999) and Siebel *et al.* (2000) presented studies of whole rock geochemistry, mineral chemical analysis and Nd, Sr and Pb isotopic data for Martin Vaz Island. Marques *et al.* (1999) studied one phonolitic sample from the island related to the Pico das Gaivotas Unit. Siebel *et al.* (2000) presented data for a basanite sample from Martin Vaz that can be related to the Bandeira Unit described here. Based on radiogenic isotopes, both works suggest that Martin Vaz rocks were generated with contribution from either depleted mantle (DMM or N-MORB) and enriched mantle (EM1 or HIMU) with minor contribution of HIMU, FOZO and C components. Nevertheless, Marques *et al.* (1999), analyzing the decoupling between Sr-Nd isotope and Rb/Sr – Sm/Nd ratios, suggested the involvement of a mantle metasomatic process with contribution of continental lithospheric mantle. Siebel *et al.* (2000) proposed the participation of oceanic lithosphere in the process due to the moderately high $^{206}Pb/^{204}Pb$ content. The aforementioned works also correlated the primitive melt generation, that evolved by fractional crystallization, to the garnet-lherzolite stability field.

Santos (2013; 2016) and Santos *et al.* (2015; 2018a) defined the evolution of Bandeira and Pico das Gaivotas Units rocks as a slow process in multiple-staged magmatic chamber, as suggested by the occurrence of millimetric zoned clinopyroxene phenocrysts presenting anhedral green-cores, sometimes brownish and yellowish cores (Fe and Al rich variations). According to these authors, the lavas from this archipelago were derived from low degree of partial melting (1-4%) of a metasomatized volatile-rich garnet-lherzolite mantle source mixed with a more primitive carbonatitic CO_2-rich magma in the sub oceanic lithosphere.

3 Whole-rock geochemistry compiled data

The lithogeochemical data here presented were compiled from Santos (2013; 2016) and Santos *et al.* (2018a) totalizing sixteen samples (MVA-01, MVA-02, MVA-03, MVA-04, MVA-05A, MVA05B, MVA-06, MVA-07, MVA-08, MVA-09A, MVA-09B, MVA-10, MVA-11, MVA-12, MVA-13 and MVA-14) from lithotypes presented in Martin Vaz main Island. CIPW norm was calculated using Hollacher's excel spreadsheets and is presented in Table 1 and used in rock classification according to Le Bas *et al.*, (1986) and criteria described in Le Maître (2005).

Bandeira Unit (BU) – Alkaline rocks from BU have SiO_2 content ranging from 38 to 40 wt.%, MgO from 8 to 15 wt.%, TiO_2 from 3 to 5 wt.% and P_2O_5 content from 0.84 to 1.69 wt. %. The samples from Bandeira unit are classified as foidite (Le Bas *et al.*, 1986; Fig. 2A). Seven samples of this unit (MVA-03, MVA-04, MVA-07, MVA-09A, MVA-09B, MVA-11, and MVA-14) are classified as melanephelinites (Santos *et al.*, 2018a), because they have less than 20% of normative nepheline and less than 5% of normative albite (Le Bas *et al.*, 1986; Table 1). Samples MVA-10, MVA-12 and MVA-13 have less than 20% of normative nepheline and more than 5% of normative albite (Table 1), containing olivine phenocrysts and classified as olivine basanite.

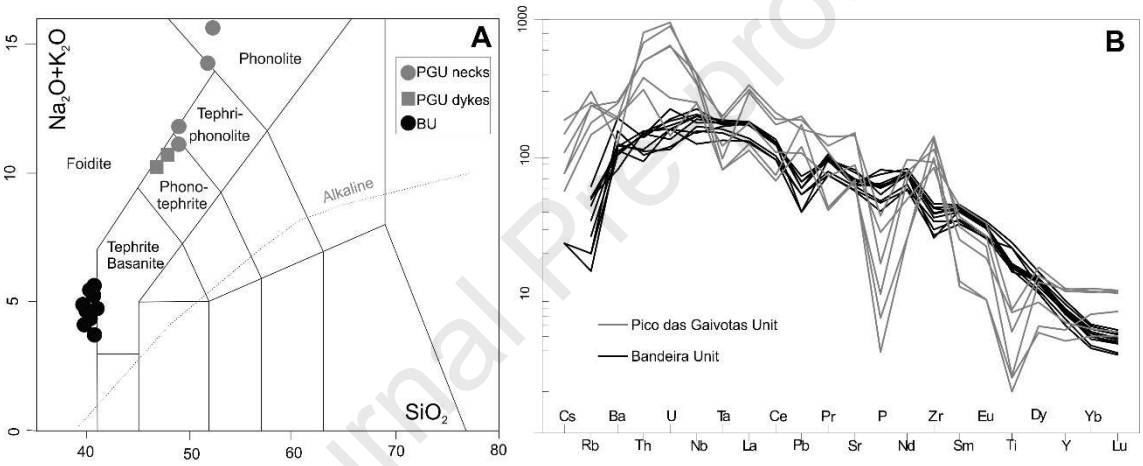

Figure 2: A) TAS classification diagram according to Le Bas *et al.* (1986). B) Multielementar diagram (normalized to primitive mantle of McDonough and Sun, 1995) for PGU and BU from Martin Vaz Island.

Pico das Gaivotas Unit (PGU) – Alkaline rocks from PGU show higher content of SiO_2 - 46 to 52 wt.% and low content of MgO ranging from 0.23 to 2.12 wt.%; TiO_2 ranges from 0.50 to 1.58 wt. % and P_2O_5 from 0.08 to 0.78 wt. %. The PGU rocks are classified as phono-tephrite/tephri-phonolite and nosean-phonolite, according to TAS diagram (Le Bas et al., 1986; Figure 2A). Multielementar diagram (Fig. 2B) shows different patterns between Bandeira Unit (BU - black lines) and Pico das Gaivotas Unit (PGU – grey lines) reflecting variations in the crystalline phases (PGU - apatite and titanoaugite, presenting P and Ti negative anomalies, for example).

Table 1 – Summarize CIPW norm for Martin Vaz rocks. Data according to Santos (2013; 2016) and Santos *et al*. (2018a).

Normative	Bandeira Unit		Pico das Gaivotas Unit	
Minerals	Melanephelinite	Olivine basanite	Tephri-phonolite/ Nosean-phonolite domes	Phono-tephrite dykes
An	5.19	12.94	2.15	12.60
Ab	0.67	7.67	15.75	11.18
Or	0.00	4.59	32.03	29.20
Ne	15.32	13.14	26.00	19.55
Lct	6.87	0.00	0.00	0.00
Di	24.73	26.89	10.97	8.04
Ol	32.79	15.94	1.91	6.38
Il	6.09	8.66	1.19	2.93
Mag	2.07	2.19	0.50	1.00
Ap	2.71	3.15	0.45	1.59
Sum	96.43	95.17	90.95	92.44

4 Materials and methods

For mineral chemistry studies, three BU melanephelinite samples (MVA-03, MVA-04 and MVA-09A) and one PGU dome sample (MVA-08) were analyzed. Core/rim differentiation was made through petrographic differences such as crystal shape, color, and texture. Analyses were made by electron microprobe technique using the ARL-SEMQ probe from North Carolina State University (NCSU) and JEOL JXA-8283 from the Universidade Federal do Rio de Janeiro (UFRJ). In the NCSU analyses, olivine, clinopyroxene, orthopyroxene, plagioclase, microcline, and chromite were used as reference minerals supported by the Smithsonian Institute in addition to Ni- containing synthetic diopside. An electron beam of 1-2 mm in diameter was used for each 10 second counting cycle per peak and bottom analyzes, operating at accelerated voltage of 15 KeV and 0.015 mA beam current. The analyzes performed at the Electronic Microprobe Laboratory of the Department of Geology of UFRJ (LabSonda) had the analytical conditions of 15 KeV voltage, 20 nA filament current and 1 mm diameter beam. Sanidine, olivine, orthopyroxene, clinopyroxene, kaersutite and ilmenite were the reference minerals used in the quantitative analyses.

For the geothermobarometry study, the less anhedral crystals, with exception of constant anhedral green (brownish)-cores were selected to achieve the most trustworthy crystal-liquid pair, nevertheless, these data are not 100% in equilibrium as showed in CPX-liquid predicted and measured in Fig. 8.

Excel® tables obtained from the Gabbrosoft's website (https://www.gabbrosoft.org/) were used to calculate end-members and FeO and Fe_2O_3 stoichiometric estimations. Molecular composition was obtained through Putirka's geothermobarometry excel table, available in http://www.fresnostate.edu/csm/ees/faculty-staff/putirka.html. Pyroxene classification is based on Morimoto *et al*. (1988).

Clinopyroxene thermobarometer was based on Putirka's P and T estimations (equations 31 for pressure and 34 for temperature; see Putirka *et al*., 2008 and Neave & Putirka, 2017 for details) which were developed for volcanic systems. This model can be used for hydrated or anhydrous ultramafic and intermediate rocks. Temperature of 1100 °C and one logarithmic unit above the quartz-fayalite-magnetite (QFM) buffer of oxygen fugacity is considered in this model. These calculations consider the jadeite molecules in the structure of clinopyroxenes and produce a standard error of ± 1.4 Kbar. Equilibrium value between crystal and liquid is assumed following values according to Roeder & Emslie (1970) of $K_D(Fe\text{-}Mg)^{cpx\text{-}liq} = 0.27 \pm 0.03$. Differences between predicted and measured DiHd, EnFs and CaTs components to Martin Vaz clinopyroxenes approaches to zero. The composition of pyroxenes was selected from those whose sum was greater than 100% with K_2O content of about 0.0 wt. % on the basis of six oxygen as presented in Longpré *et al*. (2008).

To verify clinopyroxene pressure estimates, silica-activity barometer was utilized (Putirka, 2008). The Silica activity model provides pressure values in which a primitive melt was in equilibrium with olivine + (ortho-) pyroxene, but we considered it for the clinopyroxene-olivine paragenesis. The same comparison was made with olivine-liquid thermometer (Putirka, 2007), to ratify Bandeira Unit olivine crystallization temperature.

5 Results

5.1 Petrography

5.1.1 The Bandeira Unit (BU)

This unit consists of melanephelinites and olivine basanite showing hypocrystalline matrix and porphyritic texture with phenocrysts of olivine and pyroxene showing various sizes, even though clinopyroxene phenocrysts are rare or completely absent in the olivine basanite. Olivine phenocrysts have up to 1 mm, are anhedral or subhedral, and show resorption features (Fig. 3A), poikilitic texture and a weathered film of iddingsite is present. The matrix consists of feldspars, feldspathoids (mainly nepheline), perovskite and glass (less common). The accessory minerals include titanomagnetite (as

determined by backscattering) disseminated in the matrix as micro phenocrysts or included in the olivine and pyroxene phenocrysts, characterizing a poikilitic texture.

5.1.2 The Pico das Gaivotas Unit (PGU)

PGU is characterized by tephri-phonolite/phono-tephrite and nosean-phonolite domes and phono-tephrite dykes with phenocrysts of nosean and sanidine, and micro phenocrystals of nepheline, clinopyroxene, titanite and kaersutite (Figs. 3B and 3C). The matrix is holocrystalline, composed of feldspars and feldspathoids (mainly nepheline) and show magmatic flow texture. Apatite and titanomagnetite comprise accessory minerals. Nosean crystals are hexagonal or squared, euhedral or subhedral with about 0.66 mm in size (Fig. 3D). These crystals present zeolitization, sericitization and opaque reaction rims, as well as poikilitic texture with titanomagnetite and apatite inclusions, sometimes presenting needle-like forms.

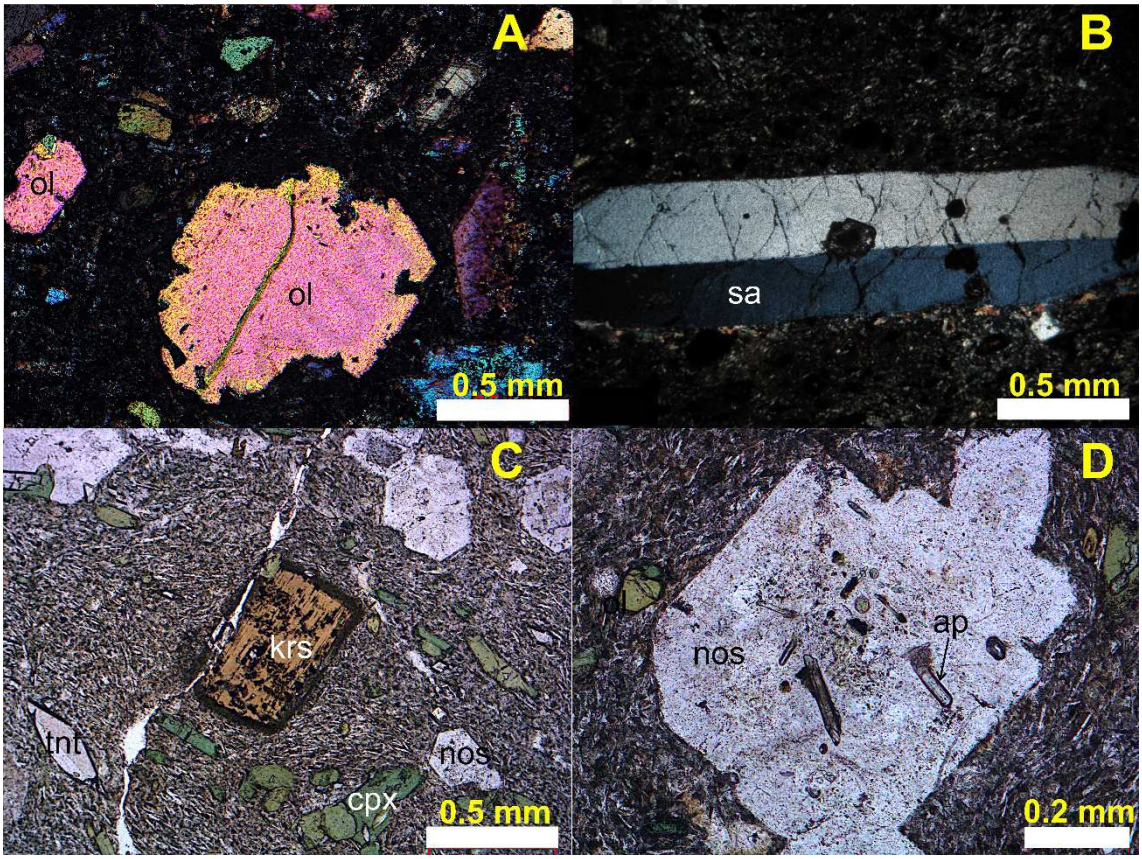

Figure 3: A) Resorbed olivine phenocrysts from Bandeira Unit melanephelinite. B) Sanidine phenocryst from phonolitic domes, Pico das Gaivotas Unit. C) PGU sample - Kaersutite phenocryst with opaque inclusions, nosean phenocrysts and cpx and titanite micro phenocrysts from nosean-phonolite neck. D) Nosean phenocryst with apatite inclusions and cpx microphenocrysts from Pico das Gaivotas phonolitic domes.

Abbreviations such as: **ol** – olivine, **sa** – sanidine, **krs** – kaersutite, **cpx** – clinopyroxene, **tnt** – titanite and **nos** – nosean. A, B crossed polarizers, C, D parallel polarizers.

Figure 4 presents Martin Vaz Archipelago geologic map modified from Santos *et al.* (2015), with the Bandeira Unit distinction in olivine basanite and melanephelinite faciological units.

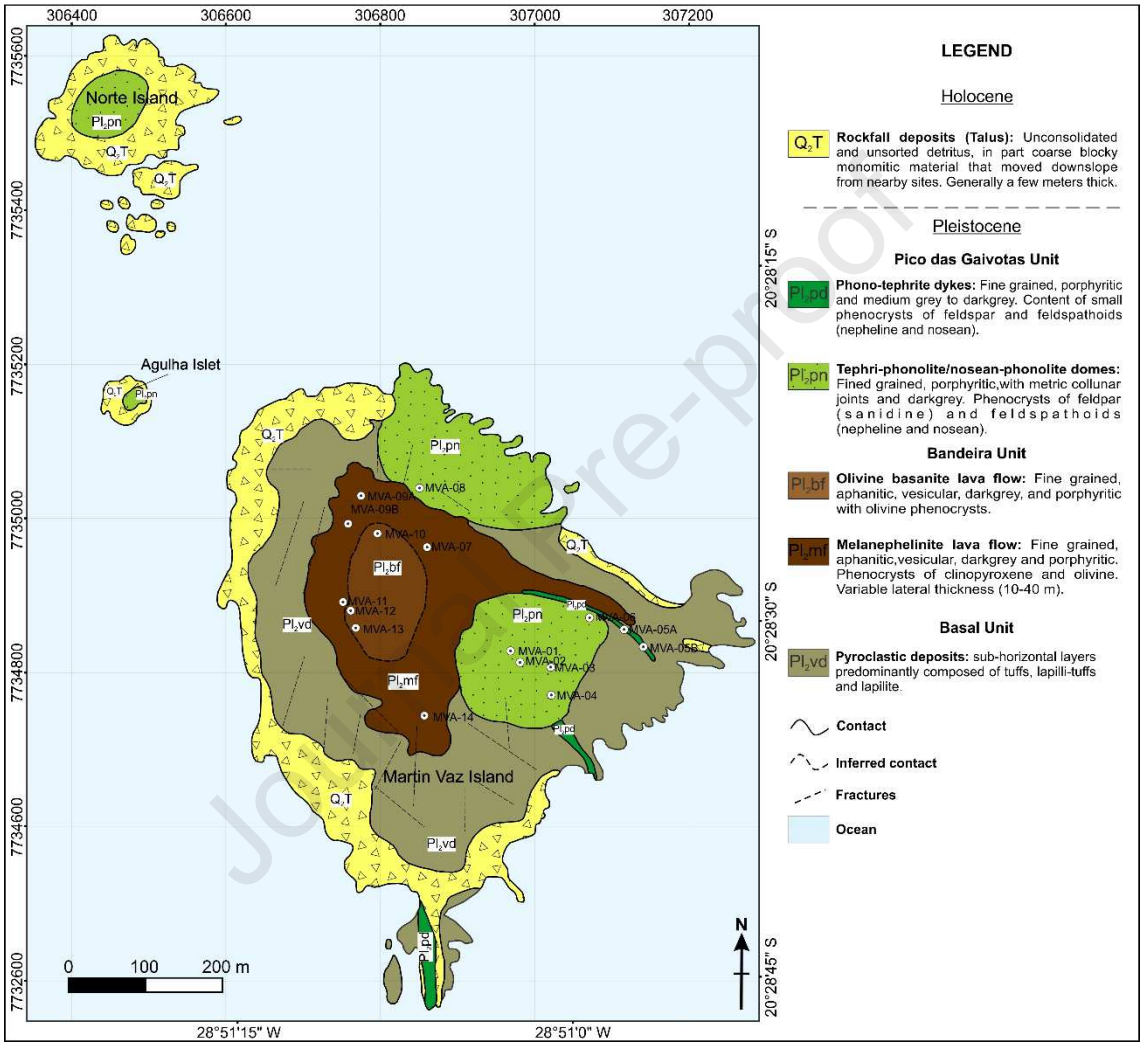

Figure 4: Martin Vaz simplified geological map modified from Santos *et al.* (2015). Olivine-basanite body was inferred by the localization of the three basanitic samples (MVA-10, MVA-12, MVA-13). Norte Island geology was made by photo interpretation.

5.1.3 Clinopyroxenes

Clinopyroxene crystals occur in a wide range of sizes and shapes, and in some of them the core-rim structure is noticeable. These cores are anhedral and show pleochroic green-core, sometimes brownish green, in average of 0.56 mm in size, with sieved and poikilitic textures containing apatite and opaque (mostly titanomagnetite) inclusions.

The crystals rims are subhedral to euhedral, presenting, sometimes, opaque replacement at the borders and magmatic resorption texture indicating crystal-liquid disequilibrium (Figs. 5A-E).

Crystals without core-rim structure often occur as strips but also faceted, euhedral or subhedral with an average size of 0.33 mm. They also show magmatic resorption and opaque replacement at the borders and they also appear, sometimes, as glomeroporphyries (Fig. 5F).

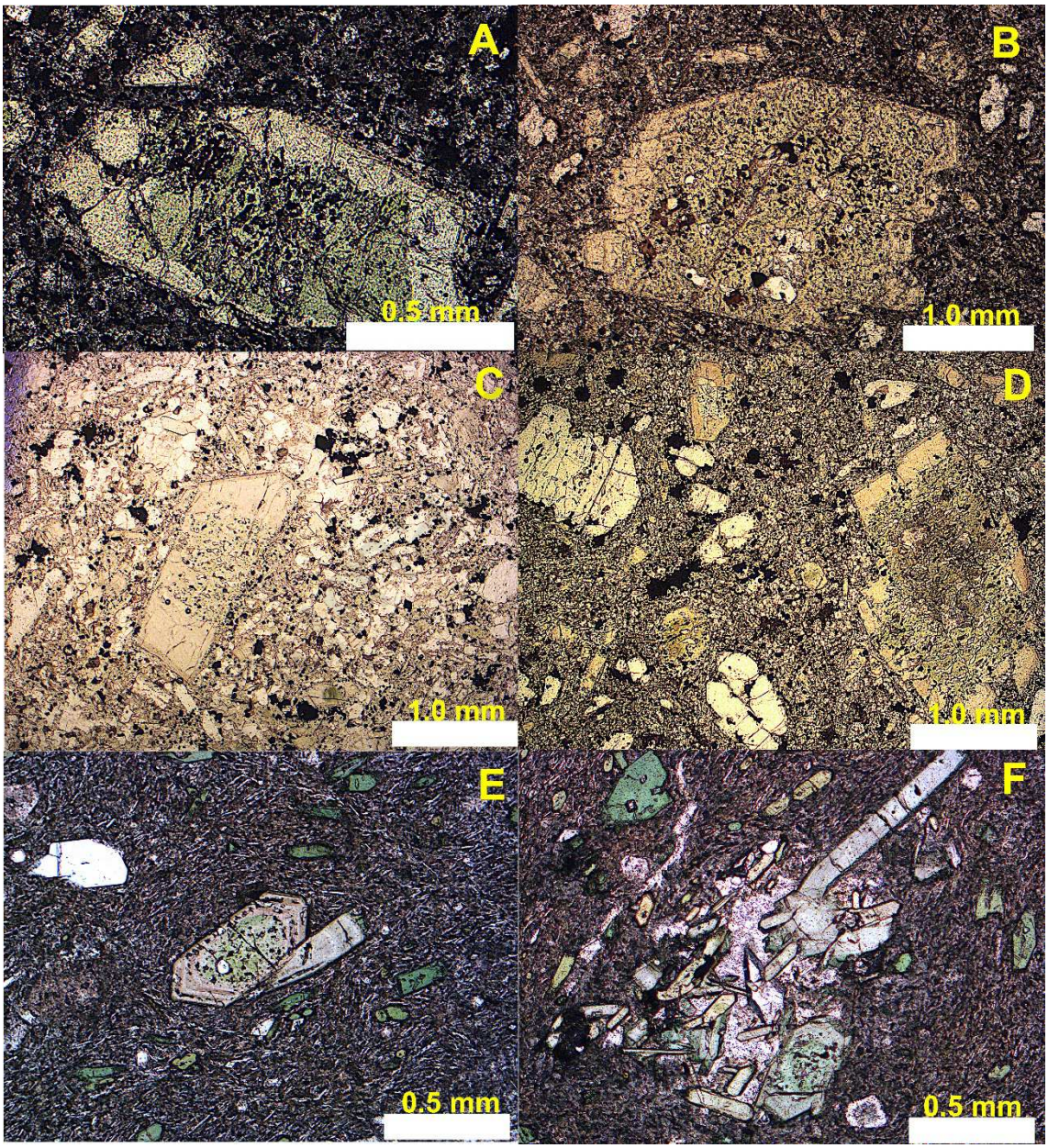

Figure 5: A) Green-core clinopyroxenes with sieved and poikilitic textures and subhedral brownish-green rims surrounded by titanomagnetite. Sample from Bandeira Unit melanephelinite. B and C) Represents green core clinopyroxenes with sieved and poikilitic textures with partial resorbed rim surrounded by titanomagnetite. Sample from Bandeira Unit melanephelinite. D) Large green-core clinopyroxene at the right, resorbed olivine phenocrysts up left and opaque micro phenocrysts scattered all over the matrix,

from Bandeira Unit melanephelinite. E) Glomeroporphyry formed, mainly, by clinopyroxenes with minor amount of green-core structures along with nepheline, titanite and opaque minerals. Sample from Pico das Gaivotas Unit phonolitic domes. F) Strongly zoned green core cpx with opaque inclusions from Pico das Gaivotas Unit nosean-phonolite domes. All photomicrographs are parallel polarizers.

5.2 Mineral Chemistry

5.2.1 Olivines

Compositions of Martin Vaz melanephelinite olivines (Bandeira Unit) have slightly differences relative to grain size. Phenocrysts show values ranging from $Fo_{80-88,}$ matrix raging from Fo_{77-85} and a macro phenocryst with Fo_{85}. Phenocrysts and macro-phenocryst have low to high NiO contents ranging from 0.00 – 0.36 wt.%. Matrix crystals present mid-low to very high content, varying from 0.07 – 0.72. CaO contents range from 0.00 to 0.71 wt.% in phenocrysts and macro phenocryst and from 0.39 to 0.86 in matrix olivines (Table 2).

5.2.2 Clinopyroxenes

Clinopyroxenes of melanephelinite rocks (BU) have green-core ($Wo_{45–51}$ $En_{18–35}$ Fs_{8-31}) composition. The rims and intermediate points (called here as crystal mantle) of these minerals have similar composition such as (Wo_{45-51} En_{32-43} Fs_{8-23}) (Fig. 6). The cores of these crystals have Mg# (100*[Mg]/[Mg + Fe]) ranging from 44.71 to 67.97, molecular Al composition ranging from 0.10 to 0.22 and Ti from 0.03 to 0.06. The crystal mantle has Mg# 69.10 to 75.51, molecular Al between 0.12 to 0.30 and Ti from 0.03 to 0.07. Finally, the crystal rims have 57.46 – 84.12 Mg#, 0.05 – 0.26 of Al and 0.03 – 0.09 of Ti (molecular Al and Ti calculated on basis of 32(O)).

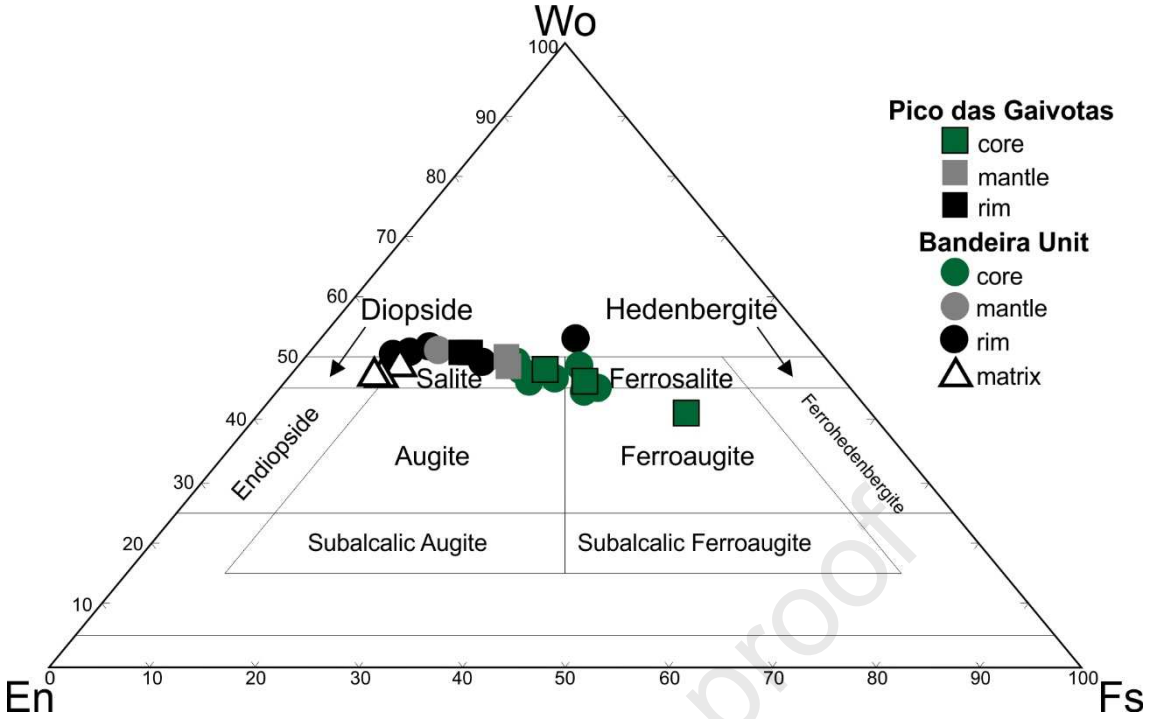

Figure 6: Clinopyroxene compositions from Bandeira and Pico das Gaivotas Units (BU and PGU) and classification according to Morimoto *et al*. (1988).

Clinopyroxenes phenocrysts of nosean-phonolite domes (PGU) also have green-core, with end-members composition of (Wo_{41-48} En_{18-28} Fs_{24-41}). Mantles and rims of these minerals show compositions (Wo_{49-51} En_{31-35} Fs_{15-19}) (Fig. 6). The cores have Mg# (43.73 – 56.14); Al (0.11 - 0.21) and Ti (0.02 - 0.06). Mantles have Mg# (62.08 - 62.19), Al (0.15 - 0.18) and Ti (0.03 - 0.04) and rims have Mg# (68.43 - 70.03), Al (0.30 - 0.33) and Ti (0.09 - 0.1). The matrix clinopyroxenes of PGU have Mg# (80.97 - 84.13), Al (0.11 - 0.26) and Ti (0.05 - 0.07). In general, all green core clinopyroxenes from Martin Vaz rocks are richer in FeO*, Na_2O, SiO_2 and poor in MgO, CaO and Al_2O_3 comparatively to the rim and mantle (Table 3; Fig. 7).

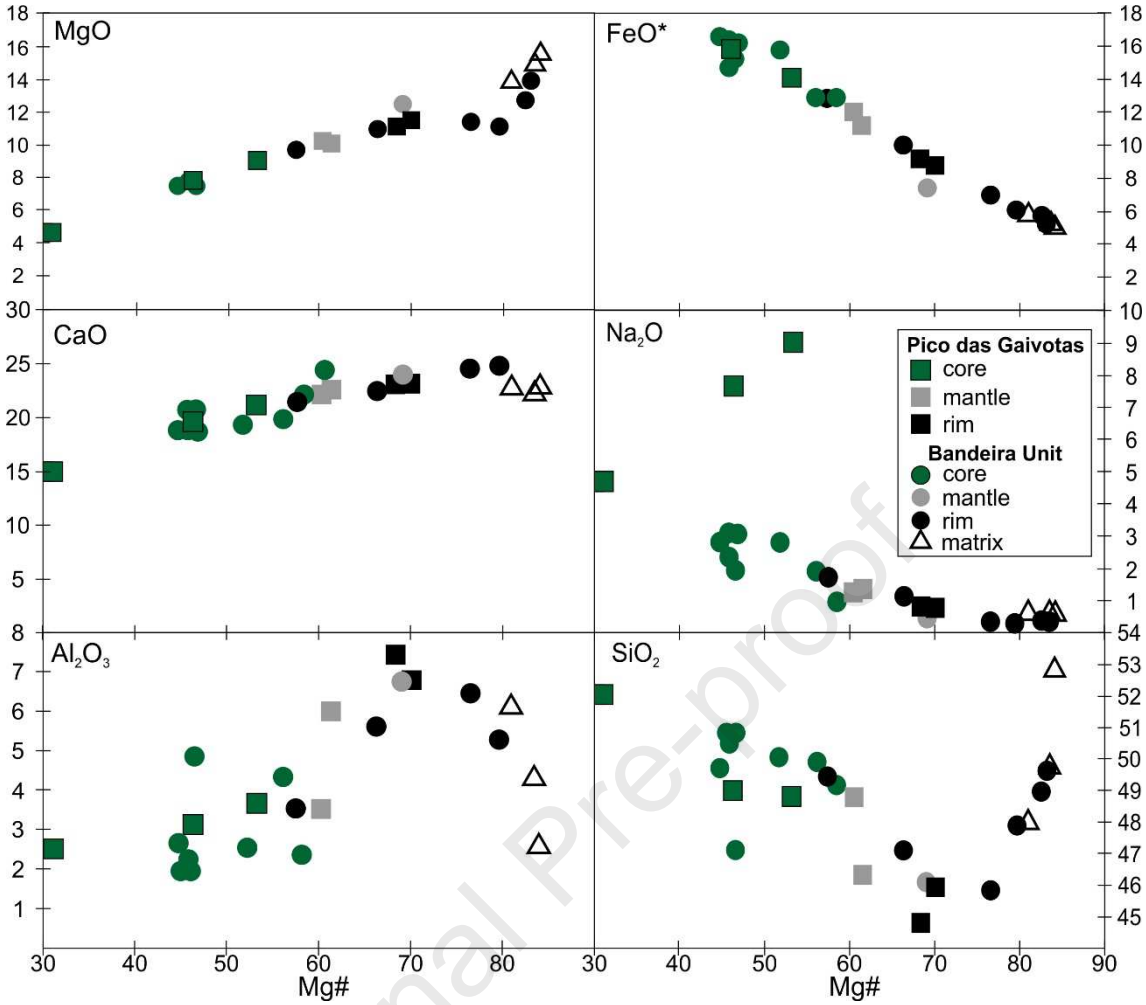

Figure 7: Bandeira Unit and Pico das Gaivotas Unit major elements (wt.%) *versus* Mg# for Martin Vaz clinopyroxene phenocrysts.

6 Geothermobarometry

The clinopyroxene-liquid equilibrium test is based on the difference between observed and predicted (by regression analyses) clinopyroxene components (Putirka, 1999; 2008), and it shows that all components (DiHd, EnFs and CaTs) from the majority of BU clinopyroxenes are near to 1:1 line (Fig. 8). However, PGU clinopyroxenes are outlying. In other words, considering 10% deviation of the line acceptable (Jeffery *et al.*, 2013), most of BU clinopyroxene analyses are near to the equilibrium with melt, making them suitable for thermobarometric calculations. In turn, PGU clinopyroxene analyses show lack of equilibrium with melt and may present erratic thermobarometer calculations. For this reason, we also used in our model a liquid from which pyroxene may have crystallized (Fig. 8; MgO *ca*. 1.56 wt.%) replacing the whole-rock composition from MVA-08 sample (MgO *ca*. 0.6 wt.%).

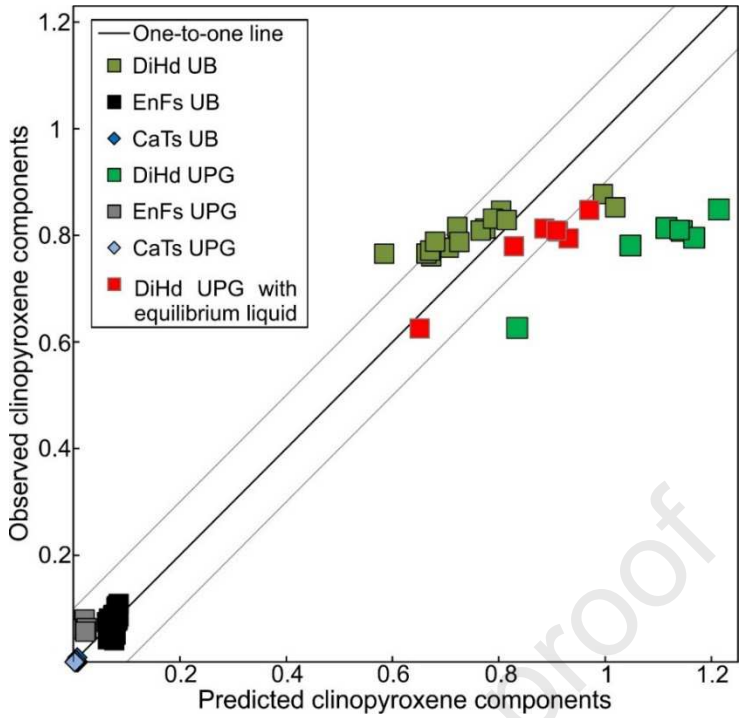

Figure 8: Clinopyroxene-liquid equilibrium test based on the difference between observed and predicted DiHd, EnFs and CaTs clinopyroxene components (Putirka, 1999; 2008). One-to-one line represents the crystal-liquid equilibrium and 10% of deviation is assumed to be acceptable (Jeffery *et al.*, 2013). All clinopyroxene analyses of both Pico das Gaivotas and Bandeira Units were used in this test. Whole rock composition was used to represent the liquid. Red points represent whole rock composition for PGU with MVA-04 liquid in equilibrium with cpx (see Supp. Material 1 and 4 for details).

Geothermobarometry data from clinopyroxene-liquid composition, using Neave and Putirka (2017) model for anhydrous base indicate pressure and temperature conditions for the BU clinopyroxenes crystallization ranging from 10.4 – 16.1 Kbar and 1265.4 – 1336.2 °C for the green-cores; 6.3 Kbar and 1178.0 °C for the mantle and -0.8 – 8.30 Kbar and 1101.9 – 1232.9 °C for the rim (Fig. 9). Silica-activity barometer (Putirka, 2008) was applied for validating the Bandeira Unit barometer and thus thermometer, once it shows pressure conditions at the moment that primitive liquid was in equilibrium with pyroxene + olivine. This barometer indicates pressure ranging from 9 – 22 Kbar for the Bandeira Unit whole rock compositions, using cpx-liquid temperature estimates for core and rim analyzes (Fig. 9 – grey field).

For the PGU, we did a correction related to the liquid used in the calculations from which the clinopyroxene must have crystallized. MVA-08 liquid has a MgO content of 0.6 wt.% and is unlike to have crystalized the observed cpx crystals. For this reason, another sample (MVA-02) liquid composition from the PGU was used (see Supp.

Material 1 excel spreadsheet for calculations purposes) in equilibrium with cpx so that the pair crystal-liquid could fall inside the equilibrium curves (Figure 8; MgO *ca*. 1.56 wt.% - MVA-02).

To testify the relations between the two samples (MVA-02 and MVA-08) a modal calculation and a fractional crystallization test by major element mass balance were made using the Petro Mode excel spreadsheet (available in http://hdl.lib.byu.edu/1877/2708; Supp. Material 4). From these tests, it was found that (i) from MVA-02 composition would be possible to crystallize a rock with the observed MVA-08 modal composition (11 to 17% of cpx), and (ii) by removing the observed mineral phases from the MVA-02 liquid composition, a rock with a similar composition of the MVA-08 would be generated. Therefore, it is acceptable that the MVA-02 composition is used to meet the crystal-liquid equilibrium requirement.

Geothermobarometer data indicate pressure and temperature conditions for the PGU clinopyroxene crystallization in equilibrium with liquid ranging from 15.7 – 24.3 Kbar and 1033.2 – 1132.6 °C for the cpx green-cores; 13.3 – 15.0 Kbar and 1004.1 – 1119.9 °C for the cpx mantles and 14.4 – 15.1 Kbar and 1015.2 – 1018.3 °C for the crystal rims (Fig. 9).

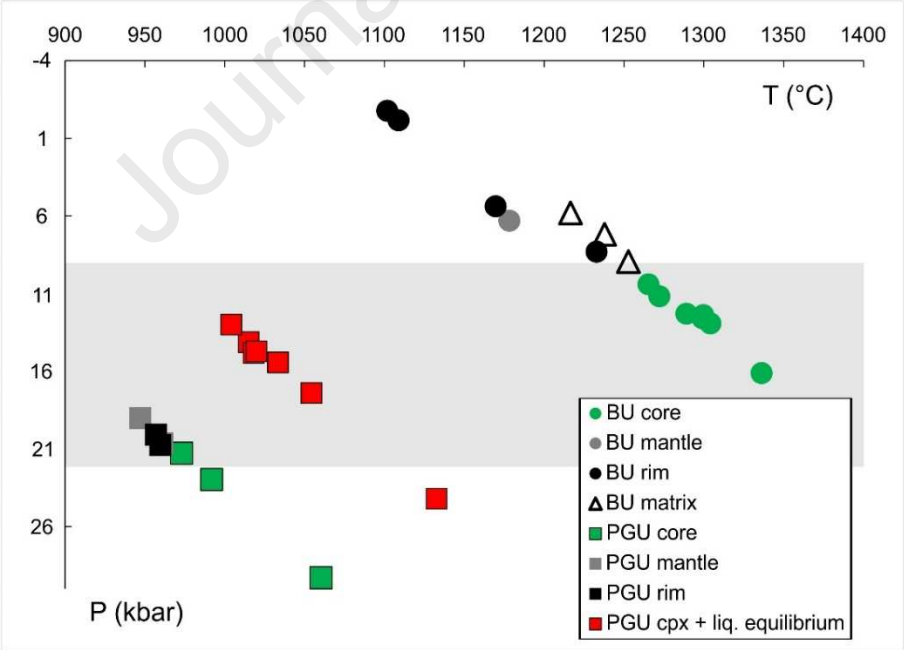

Figure 9: P and T estimates for clinopyroxene crystallization from their composition in equilibrium with melt, according to Neave and Putirka (2017). Grey area represents Si-activity pressure range to Bandeira Unit rocks (Putirka, 2008). In red, P-T recalculations for the Pico das Gaivotas Unit using a new liquid from MVA-02 from which cpx crystallized (MgO *ca*. 1.56 wt.%).

Table 2: Olivine composition table (one point per sample) from microprobe analysis with end members and crystallization temperature estimates according to Putirka (2007).

	MVA-04 (BU)				MVA-09A (BU)							
	phenocryst	**phenocryst**	**phenocryst**	**phenocryst**	**phenocryst**	**phenocryst**	**phenocryst**	**macro phenocryst**	**matrix**	**matrix**	**matrix**	**matrix**
SiO_2	39.17	39.01	39.47	39.01	40.72	40.49	40.23	39.27	39.86	39.82	40.11	39.32
Al_2O_3	0.02	0	0	0.01	0	0	0	0	0	0	0	0
FeO	17.19	17.38	16.29	16.62	11.65	12.80	15.75	13.63	17.00	19.57	13.85	17.04
MnO	0.33	0.34	0.19	0.31	0.19	0.26	0.30	0.25	0.55	0.70	0.28	0.48
MgO	42.57	41.62	43.33	42.07	46.61	46.46	44.47	45.37	42.18	39.63	45.39	42.57
CaO	0	0.7	0.40	0.71	0.29	0.32	0.25	0.47	0.73	0.86	0.39	0.54
Cr_2O_3	0.01	0	0.01	0	0	0	0	0	0	0	0	0
NiO	0.02	0.02	0	0.04	0.31	0.33	0.21	0.36	0.18	0.07	0.25	0.72
Total	99.34	99.08	99.71	98.79	99.79	100.69	101.23	99.37	100.53	100.69	100.29	100.69
Fo	81.23	80.71	82.40	81.57	87.51	86.37	83.15	85.34	81.06	77.69	85.12	81.23
Fa	18.39	18.90	17.38	18.08	12.27	13.34	16.52	14.38	18.32	21.51	14.57	18.23
Tp	0.36	0.37	0.21	0.34	0.21	0.28	0.32	0.26	0.60	0.78	0.30	0.53
T (°C)	1387	1377	1384	1303	1389	1392	1318	1379	1400	1417	1397	1412

Table 3a: Clinopyroxene composition table from microprobe analysis with end members calculation. Continue to the next page.

	MVA-03 (BU)								MVA-09A (BU)			
	core	**core**	**core**	**core**	**core**	**core**	**rim**	**rim**	**core**	**matrix**	**matrix**	**matrix**
SiO_2	47.11	49.74	50.76	50.76	50.07	50.53	49.46	47.09	49.93	48.06	49.71	52.82
TiO_2	2.17	0.92	0.56	0.60	0.68	0.62	0.97	2.48	0.89	2.43	2.32	1.69
Al_2O_3	4.86	2.67	2.24	2.21	2.47	2.49	3.52	5.63	4.44	6.09	4.30	2.57
FeO*	15.26	16.55	16.29	16.04	15.74	14.68	12.79	9.95	12.86	5.79	5.22	5.08
MnO	0.02	0	0	0	0	0	0	0	0.53	0.08	0.09	0.10
MgO	7.46	7.51	7.73	7.87	7.68	8.83	9.69	10.98	9.24	13.84	14.88	15.53
CaO	20.56	18.84	18.79	18.94	19.36	20.5	21.34	22.54	19.87	22.78	22.30	22.79
Na_2O	1.94	2.81	3.09	3.00	2.81	2.32	1.74	1.13	1.89	0.59	0.57	0.55
Cr_2O_3	0.02	0	0.01	0.01	0	0	0.02	0	0.03	0.45	0.04	0
NiO	0.02	0	0	0	0	0.01	0	0.03	0	0	0	0
ZnO	0.03	0.09	0.04	0.08	0.07	0	0.01	0	0	0	0	0
Total	99.50	99.18	99.54	99.55	98.91	100.01	99.58	99.86	99.69	100.16	99.46	101.17
Wo	48.14	44.88	44.70	44.89	45.95	46.53	45.27	49.54	46.45	48.93	47.31	47.13
En	24.32	24.89	25.60	25.97	25.39	27.89	31.55	33.60	30.05	41.31	44.00	44.65
Fs	27.52	30.22	29.68	29.12	28.65	25.57	23.16	16.84	23.50	9.73	8.67	8.25

Table 3b: Clinopyroxene composition table from microprobe analysis with end member calculation.

	MVA-04 (UB)							MVA-08 (UPG)						
	core	**mantle**	**rim**	**rim**	**rim**	**rim**	**rim**	**core**	**core**	**core**	**mantle**	**mantle**	**rim**	**rim**
SiO_2	49.19	46.05	47.90	45.85	49.61	48.97	45.88	49.01	48.88	52.84	48.78	46.32	44.80	45.9
TiO_2	0.91	2.48	2.28	3.20	2.18	1.86	2.84	1.11	1.20	0.79	1.47	2.53	3.45	3.01
Al_2O_3	2.43	6.77	5.28	6.46	3.46	4.20	7.20	3.15	3.65	2.42	3.50	6.02	7.40	6.78
FeO	12.84	7.23	6.07	6.97	5.22	5.51	6.88	15.86	14.12	19.66	11.97	11.26	9.15	8.73
MnO	0	0.04	0	0	0	0.02	0.04	0	0.01	0	0	0	0	0
MgO	10.15	12.52	13.95	12.74	14.45	14.60	12.84	7.68	9.03	4.68	10.24	10.05	11.12	11.45
CaO	22.17	24.01	24.77	24.57	24.45	24.70	24.35	19.6	21.15	15.07	22.16	22.52	23.11	23.13
Na_2O	0.99	0.47	0.29	0.34	0.34	0.38	0.41	2.37	1.89	4.05	1.22	1.32	0.76	0.76
Cr_2O_3	0	0.36	0.04	0.04	0.02	0.23	0.22	0.02	0.01	0	0.03	0.01	0	0.01
NiO	0.02	0	0	0.01	0	0	0	0	0	0	0.01	0.03	0	0
ZnO	0.05	0	0.01	0.01	0.13	0.04	0	0	0	0.09	0	0.05	0	0.01
Total	98.78	99.97	100.63	100.22	99.90	100.55	100.69	98.91	99.99	99.62	99.41	100.16	99.81	99.88
Wo	47.98	51.04	50.67	51.54	50.29	50.11	51.20	46.23	47.46	40.91	48.55	49.87	50.64	50.49
En	30.56	37.03	39.73	37.18	41.37	41.21	37.57	25.13	28.21	17.68	31.21	30.98	33.93	34.79
Fs	21.44	11.91	9.58	11.26	8.33	8.66	11.21	28.63	24.32	41.40	20.22	19.14	15.42	14.70

7 Discussion

7.1 Mineral chemistry correlation and Martin Vaz rocks evolution

Santos *et al.* (2018a) suggested that Martin Vaz magmas have suffered volatile-rich melts and/or carbonatitic liquid influence on their genesis, which was also responsible for the formation of secondary mineral phases (e.g. apatite, kaersutite and phlogopite). Siebel *et al.* (2000) also suggested that titanite crystallization in Trindade and Martin Vaz phonolitic rocks must be responsible for the relative enrichment in HFSE and MREE and a concave downward in REE patterns. La/Sm and Sm/Yb ratios suggest that these magmas were generated by low degree partial melting in the garnet lherzolite field, as showed by Santos *et al*. (2018a).

Martin Vaz Archipelago's olivines are highly magnesian (Fo_{77-88}) and are not related to the green-core clinopyroxenes. Most of them have relatively high CaO contents (> 0.2 wt.%) that are considered to be a near-primary assemblage in equilibrium with mantle peridotites that crystallized at the beginning of magmatic differentiation (Kamenetsky *et al*., 1995; Di Battistini *et al*., 1998). However, most of them have low Cr_2O_3 and NiO contents to be related to mantle olivines. Only crystals with > Fo_{86} have NiO contents *ca*. 0.4 wt.% are consistent with the mantle olivine array defined by Takahashi *et al*. (1987).

The olivine equilibrium curve with primitive melts (Fig. 10 – Rhodes *et al.*, 1979) shows that the analyzed liquid (whole-rock composition *ca*. MgO 14 wt.%) would be in equilibrium with olivine phenocrysts with higher Fo content (Fo_{85-87}) instead of olivine crystals with lower Fo content (Fo_{77-83}). These relationships, together with the variated NiO content, may suggest that these crystals have a hybrid origin (Xu *et al*., 2003) from the highest magnesian phenocrysts, and are probably mantle xenocrysts. The phenocryst and matrix crystals disposition in the figure 10, however, represents chemical variation related to factional crystallization. Thus, these evidences point to a magma replenishment of a primitive magma, that could give a false idea of equilibrium for the highest magnesian olivines.

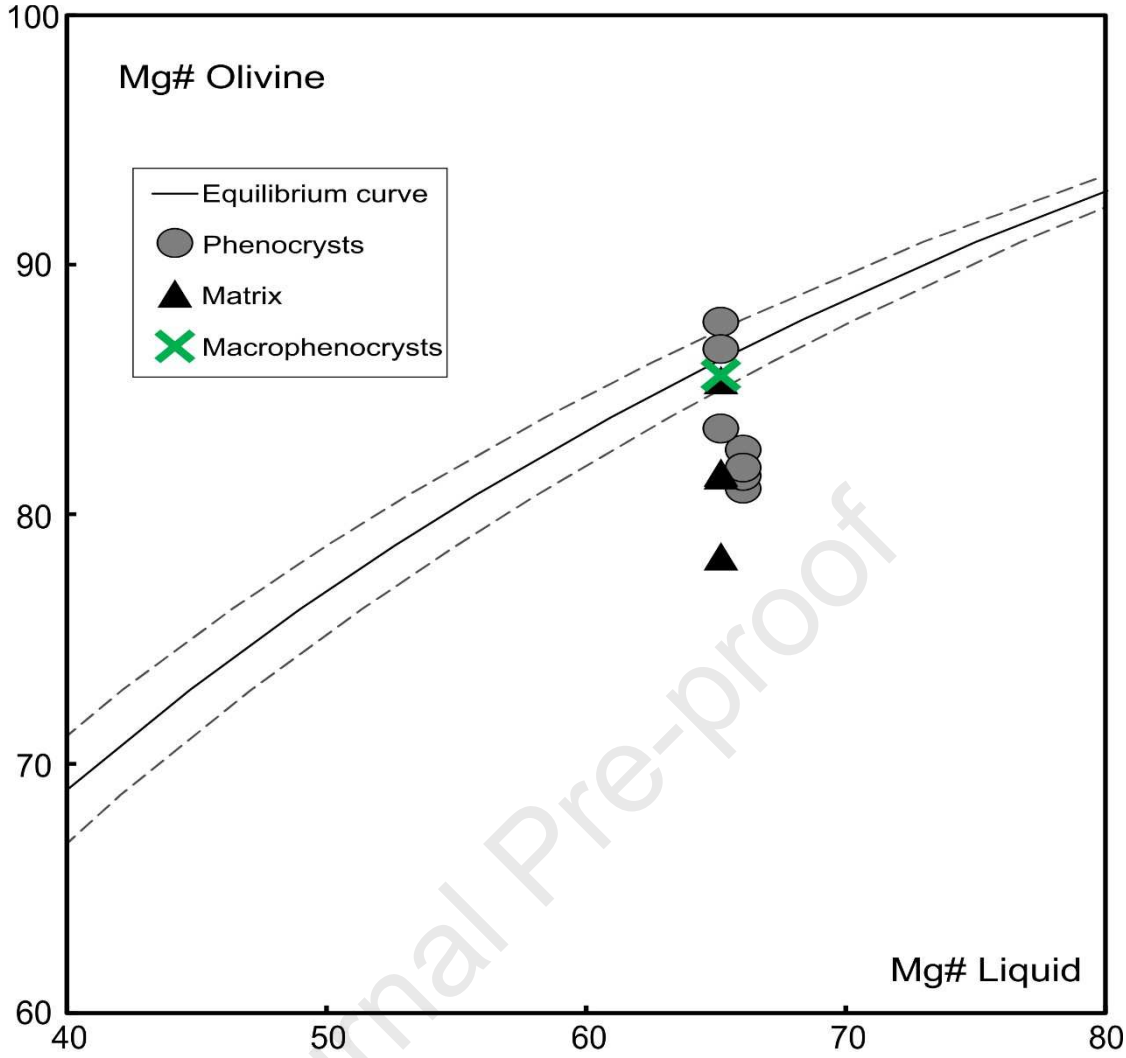

Figure 10: Fo contents of Martin Vaz olivine phenocrysts and matrix against whole rock Mg# values from Bandeira Unit, samples (MVA-04 and MVA-09A). Dashed lines denote the equilibrium curves between olivines and melt (after Putirka, 2007) calculated by using a $Fe/Mg^{ol/liq}$ taken from Roeder and Emslie (1970) and Rhodes *et al.* (1979).

7.2 Cpx mineral chemistry and geothermobarometry

The contents of Al^{VI} and Al^{IV} are an important key to evidence differences in pressure conditions in green-core clinopyroxenes relative to the mantles and rims. Martin Vaz green-cores Al^{VI} and Al^{IV} contents are plotted into the Ca-Tschermak's molecule (Ts: $CaAl_2SiO_6$; Fig. 12) field, that is a high-pressure environment (Dobosi and Fodor, 1992), opposing to the mantles and rims that are plotted into the low-pressure field of igneous rocks ("A" limit as defined by Aoki & Kushiro, 1968; Fig. 11). However, the Al^{IV} content of Martin Vaz clinopyroxenes are lower than Al^{IV} content of Colúmbia Seamount clinopyroxenes from the same volcanic ridge related to the Trindade Plume (Fig. 11A), but green-cores of Martin Vaz cpx have a similar Al^{VI} content from Colúmbia phenocrysts. Al/Ti ratios support these differences in the P values as observed

in Fig. 11B. Green-core Al/Ti ratios plot around the line limit 0.25 (mostly lower than 0.25) while rims Al/Ti ratios are more scattered but tend to plot between 0.25 and 0.5 lines and are, in general, richer in Al and Ti (Fig. 11B), but in a disperse behavior that is consistent with variations in the thermobarometer data (Fig. 9).

Beyond that, thermobarometric data indicate higher P and T conditions involved during core crystallization. Santos (2016) suggests multistage crystallization during the ascension of Martin Vaz magmas, evidenced by variation of P and T values of cpx cores, mantles, rims and as well those of the matrix. Dobosi & Fodor (1992) reported the occurrence of green core clinopyroxenes with similar aforementioned features and chemical contents, defining them as from a xenocrystic origin.

The green-core clinopyroxenes analyzed in Martin Vaz Island have lower Mg# relative to the rim and mantle crystals, that indicate the input of a more primitive liquid in the magmatic chamber being supported by the resorption texture in olivine crystals. The observed microscopic features such as sieved and resorption textures support this latter statement. Santos (2016) suggests that the disequilibrium features occurred due to a hotter and more primitive magma injection. Such injections caused changes in the total liquid composition, temperature, pressure, and oxidation state (Pearce & Kolisnik, 1990) and cause the crystallization of clinopyroxenes alternating growth/dissolution (see Dobosi & Fodor, 1992 for discussions).

Lower Fe^{3+}/Fe^{2+} ratios in the green-cores (Fig. 11C) can indicate an increase in fO_2 that is supported by the decreasing in Si/Al ratios observed in the clinopyroxene rims and mantles (Fig. 11D), as suggested by Mollo & Vona (2014) experiments. The substitution for titanomagnetite in the outer crystals rims also indicates an increase in fO_2 and an oxidized environment. This increase in oxygen fugacity corroborates with the idea of magma mixing contribution as process responsible to the Al-Ca-Fe^{3+}-Ti-rich rims crystallization.

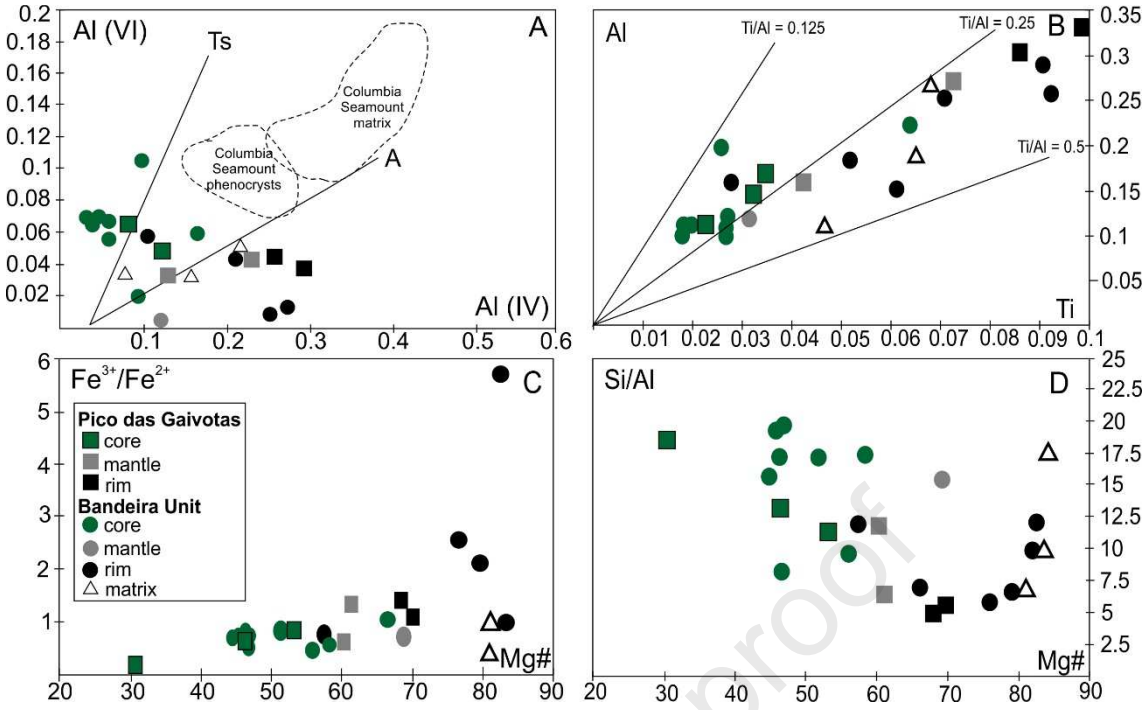

Figure 11: A) Atomic proportion of $Al^{(VI)}$ and $Al^{(IV)}$ in comparison with Colúmbia Seamount clinopyroxenes (data from Santos, 2016). Ts line represents the Ca-Tschermak's molecule ($CaAl_2SiO_6$) which is a high-pressure field. The line A represents the limit of igneous pressure environment (Aoki & Kushiro, 1968). B) Atomic $Al_{(total)}$ *versus* Ti; lines represent Ti/Al ratios. C and D) Respectively, Fe^{3+}/Fe^{2+} and Si/Al ratios against Mg#.

The equilibrium diagram (Fig. 12; Rhodes *et al.*, 1979) shows a progressive approximation to the melt equilibrium from green core to rims and cpx presented in the matrix (microphenocrysts) in BU. In PGU domes, however, the cores are closer to the equilibrium because these rocks became more evolved after rims crystallization, probably caused by a longer residence time of the magma in the chamber, that could have caused the evolution by fractional crystallization, even with the primitive magma replenishing such as suggested by Mg# content in clinopyroxenes (core *ca*. 30 and rim *ca*. 70). Regarding to this equilibrium relationship, we suggest that after green-core crystallization, a more primitive and Ca-rich liquid entered in the storage causing resorption and sieved textures (Fig. 5). Afterwards, mantle and rim were crystallized with progressively enrichment in Mg# values caused by diffusional re-equilibration between Fe and Mg (Chen *et al.*, 2018).

On the other hand, PGU rocks have MgO 0.6 wt.% (Santos *et al*., 2018a), a very low MgO content to crystallize cpx with the observed composition. Analyzing the equilibrium test (Fig. 9), cpx from PGU rocks are outlining the one-to-one curve,

indicating that these crystals crystallized from a different liquid, with at least MgO *ca*. 1.56 wt.%.

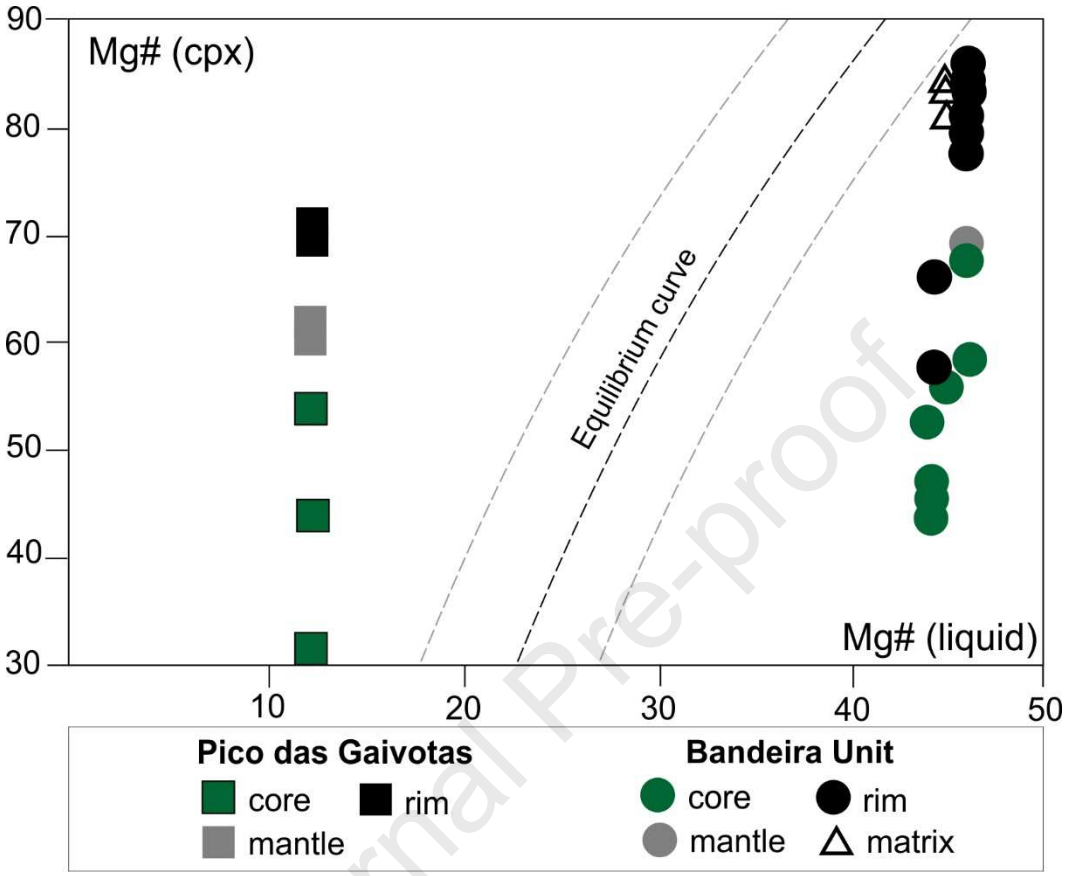

Figure 12: Mg# values in clinopyroxene phenocrysts and matrix *versus* Mg# liquid values for Martin Vaz rocks (points with ~12 Mg# (liquid) is from PGU samples). Dashed lines (after Rhodes *et al*., 1979) denote the equilibrium curves between clinopyroxenes and melt that calculated by using a $Fe/Mg^{cpx/liq}$ K_D of 0.26 ± 0.05 (Akinin *et al*., 2005).

7.3 Evolution of magma chamber model

The lower Na contents in mantles and rims can be explained by competition for Na with other groundmass mineral phases like nepheline and feldspars during crystallization such as suggested by Dobosi & Fodor (1992). Mark *et al*. (2010), however, suggested that the percolation of sodium-rich metasomatic fluid in garnet-lherzolite source can produce green-core clinopyroxenes rich in iron with up to 20% of aegirine component. Jung *et al*. (2006) reported the origin of green-cores in pyroxenes with deep-level crustal contamination and that higher content of Fe, Al, Na and Ti/Al ratios are indicative of high-pressure and that the studied case indicates deep crust storage and polybaric differentiation (Duda & Schmincke, 1985).

The chemical composition of Martin Vaz clinopyroxene phenocrysts are similar in each unit, indicating that they had the same sort of magmatic process, such as polybaric fractionation. It can be said, according to geothermobarometry data (Fig. 9), that these minerals crystallized in variable depth and, consequently, variable pressures and temperatures. Furthermore, olivine-liquid geothermometers indicates that these minerals crystallized at ~1448.6 °C (Putirka *et al.*, 2007 – Table 2), in agreement with cpx-liquid thermobarometer. Silica-activity barometer is also in agreement with cpx-liquid model, reveling 9 – 23 Kbar for BU (Fig. 9).

The high-pressure environment for PGU cpx suggests that these crystals crystallized in a variable depth range and evolved by fractional crystallization with a longer residence period in the magmatic chamber enabling strong chemical modifications.

According to the petrography and chemical characteristics of Martin Vaz rocks it is possible to estimate a model for genesis and evolution of their magmas. Olivine crystals in Bandeira Unit have distinct compositions related to size variation (micro, pheno and macro phenocrysts – Table 2). According to the petrographic analyses, the macro phenocrysts show occasionally magmatic resorption, indicating instability due to disequilibrium with the liquid (Fig. 3A and Fig. 10). Green-core clinopyroxene crystals with disequilibrium texture surrounded by opaques (Ti-magnetite) and their brownish pleochroic rims represent chemical distinction between more evolved fassaitic cores and less evolved rims such as discussed throughout the text, indicating a physicochemical change in the system.

These characteristics suggest a history of magma replenishing in multiple-staged magmatic chamber. The green-core clinopyroxenes have a genesis related to a more evolved magma in disequilibrium with a more primitive liquid that replenished the magmatic chamber. This event has caused the strong resorption of the cores and then favored the crystallization of Mg# richer rims, in which the composition is similar to the clinopyroxenes micro phenocrysts presented in the matrix (Fig. 13).

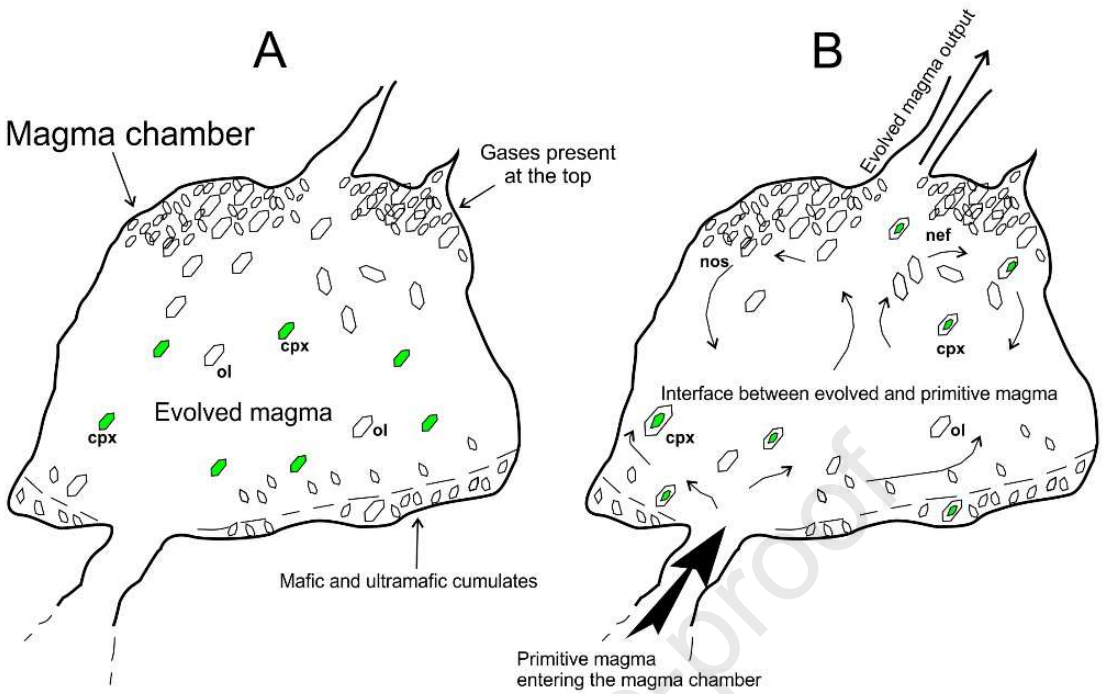

Figure 13: A) First green-core clinopyroxene crystallization stage from an evolved magma. B) Input of primitive magma into the magma chamber that originated the clinopyroxene rims and, possibly, other mineral phases from fractional crystallization, until the equilibrium with phonolitic liquid composition is reached (modified from Fodor *et al.*, 1993).

The data presented in this work show a complex evolutionary history for Martin Vaz magmas, involving polybaric crystallization, magma mixing and solid phase resorption, as well as fractional crystallization and density differentiation that is probably responsible for the faciological variation of melanephelinite and olivine basanite lava flows.

8 Concluding remarks

The Martin Vaz Archipelago magmas have a complex evolutionary history recorded in mineral and whole-rock chemistry. The island comprises a variety of lithologies such as melanephelinites, olivine basanite, phono-tephrite, tephri-phonolite and nosean-phonolite. Analyzing mineral chemistry and petrographic features such as sieved and poikilitic textures, resorption and compositional zoning, we can conclude some topics from this geological history:

(1) Bandeira Unit has reliable thermobarometer data, as shown by the predicted and observed component equilibrium tests. However, Pico das Gaivotas Unit

clinopyroxenes are in disequilibrium with the analyzed liquid and must have crystallized from a different liquid with MgO > 1.56 wt.%. Therefore, PGU clinopyroxenes have a xenocrystic origin from a less evolved liquid such as calculated previously (MgO - 1.56 wt.%).

(2) Olivine phenocrysts (> Fo_{86}) have chemical composition like a near-primary assemblage in equilibrium with mantle peridotites. They are not in equilibrium with the analyzed liquid and must have been crystallized from more differentiated magmas.

(3) Green-core clinopyroxenes have higher Al^{VI} content and lower Ti/Al ratios than rims, characteristics that are in agreement with thermobarometer data, indicating that the green-cores crystallized in higher pressure conditions. These different pressure conditions configure polybaric crystallization events to Martin Vaz rocks, and the variation range in crystallization pressure and temperature conditions suggest that crystallization followed magma ascent.

(4) Fe^{3+}/Fe^{2+} and Si/Al ratios suggest an increase of fO_2 from core to rim, probably caused by the input of a primitive Al-Ca-Fe^{3+}-Ti-rich liquid in the magmatic chamber.

(5) Green core clinopyroxenes probably crystallized from an evolved magma that must have suffered episodic magma mixing events, according to the observed zoning patterns in minerals, mostly feldspar and some euhedral clinopyroxene phenocrysts, in different mantle and crustal levels. The mixing (or the replenishment of the magmatic chamber) is responsible for the observed disequilibrium features, marked by resorption, lack of growth and compositional zoning, poikilitic and sieved textures, among others.

9 Acknowledgments

The authors thank the CNPq (Pro Trindade Program) for supporting this research (Process Nº. 557146/2009-7), and the logistic support of the Brazilian Navy. The present work is linked to the MCT/CNPq project n° 26/2009, under the coordination of researchers from Universidade do Estado do Rio de Janeiro (UERJ) and cooperation with Universidade Federal do Rio de Janeiro (UFRJ). We thank Universidade do Estado do Rio de Janeiro for PROCAD Program (Capacitation Program) leave and CAPES (Process 88881.177228/2018-01) for the post-doctorate fellowship to execute part of this research in the Aveiro University, Portugal. We thank funding from FAPERJ

(APQ1 2019 n 210.179/2019). Our many thanks to Dr. Ronald Fodor (North Carolina State University), Dr. Julio Mendes and technicians Amanda Tosi and Iara Déniz Ornellas (LabSonda- UFRJ) for analyzing the thin sections and enlightening the research. We also thanks Dr. Sérgio Wilians Oliveira Rodrigues (UFG) for the assistance with localization figure. The authors are also grateful for the critical review, illuminating suggestions and helpful comments received from the Editor and the referees, Dr. Julio Mendes and anonymous reviewer. We also thank PROCIÊNCIA project 2020 developed by Dr. Anderson Costa dos Santos as part of his personal research that donated samples to our manuscript development.

10 References

Amante, C. & B. W. Eakins., 2009. ETOPO1 1 Arc-Minute Global Relief Model: Procedures, Data Sources and Analysis. *NOAA Technical Memorandum NESDIS NGDC-24*. 19 pp.

Aoki, K. I., & Kushiro, I. 1968. Some clinopyroxenes from ultramafic inclusions in Dreiser Weiher, Eifel. *Contributions to Mineralogy and Petrology.* 18(4) :326-337. DOI: https://doi.org/10.1007/BF00399694

Akinin, V. V., Sobolev, A. V., Ntaflos, T., & Richter, W. 2005. Clinopyroxene megacrysts from Enmelen melanephelinitic volcanoes (Chukchi Peninsula, Russia): application to composition and evolution of mantle melts. *Contributions to Mineralogy and Petrology.* 150(1) :85-101. DOI: https://doi.org/10.1007/s00410-005-0007-x

Aurisicchio, C., Federico, M. & Gianfagna, A. 1988. Clinopyroxene chemistry of the high potassium suite from Alban hills, Italy. *Contributions to Mineralogy and Petrology*. 89:1-19. DOI: https://doi.org/10.1007/BF01226259

Barberi, F., Bizouard, H., & Varet, J. 1971. Nature of the clinopyroxene and iron enrichment in alkalic and transitional basaltic magmas. *Contributions to Mineralogy and Petrology*, 33(2): 93–107. DOI: https://doi.org/10.1007/bf00386108

Barton, M. & Bergen, V. M. J. 1981. Green clinopyroxenes and associated phases in a potassium-rich lava from the Leucite Hill, Wyoming. *Contributions to Mineralogy and Petrology.* 77:101-114. DOI: https://doi.org/10.1007/BF00636514

Chen, Long & Zheng, Yong-Fei & Zhao, Zi-Fu. 2018. Geochemical insights from clinopyroxene phenocrysts into the effect of magmatic processes on petrogenesis of intermediate volcanics. *Lithos.* 316-317. DOI: https://doi.org/10.1016/j.lithos.2018.07.014

Cordani, H. G. 1970. Idade do vulcanismo do Oceano Atlântico Sul. *Boletim do Instituto de Geociências e Astronomia (IGA-USP).* 1 :9-75.

Di Battistini, G., Montanini, A., Vernia, L., Bargossi, G. M., & Castorina, F. 1998. Petrology and geochemistry of ultrapotassic rocks from the Montefiascone Volcanic Complex (Central Italy): magmatic evolution and petrogenesis. *Lithos*. 43(3) :169-195. DOI: https://doi.org/10.1016/S0024-4937(98)00013-9

Dobosi, D. & Fodor, R.V. 1992. Magma fractionation, replenishment, and mixing as inferred from green-core clinopyroxenes in Pliocene basanite, southern Slovakia. *Lithos.* 28 :133-150. DOI: https://doi.org/10.1016/0024-4937(92)90028-W

Duda, A., & Schmincke, H.-U. 1985. Polybaric differentiation of alkali basaltic magmas: evidence from green-core clinopyroxenes (Eifel, FRG). *Contributions to Mineralogy and Petrology.* 91(4) :340–353. DOI: https://doi.org/10.1007/BF00374690

Fodor, R.V., Dobosi, G. & Sial, A.N. 1995. Zoned clinopyroxenes in alkali basalt: clues to fractionation and magma-mixing histories for seemingly primitive magmas. *Chemie der Erde.* 55 :133-148.

Holm, P.M. 1982. Mineral chemistry of potassic lavas of the Vulsini district. The Roman province. *Mineralogical Magazine.* 46 :379-386. DOI: https://doi.org/10.1180/minmag.1982.046.340.14

Jeffery, A.J., Gertisser, R., Troll, V.R., Jolis, E.M., Dahren, B., Harris, C., Chadwick, J.P., 2013. The pre-eruptive magma plumbing system of the 2007–2008 dome-forming eruption of Kelut volcano, East Java, Indonesia. Contrib. Mineral. Petrol. 166 (1), 275–308. DOI: https://doi.org/10.1007/s00410-013-0875-4

Jung, C., Jung, S., Hoffer, E., Berndt, J., 2006. Petrogenesis of tertiary mafic alkaline magmas in the Hocheifel, Germany. *Journal of Petrology*, 47:1637–1671. doi: https://doi.org/10.1093/petrology/egl023

Kamenetsky, V., Métrich, N., & Cioni, R. 1995. Potassic primary melts of Vulsini (Roman Province): evidence from mineralogy and melt inclusions. *Contributions to Mineralogy and Petrology*. 120(2) :186-196. DOI: https://doi.org/10.1007/BF00287116

LeBas, M.J. *et al.* 1986. A chemical classification of volcanic rocks based on the total alkali-silica diagram. *Journal of Petrology*. 27 :745-750. DOI: https://doi.org/10.1093/petrology/27.3.745

LeBas, M.J. 1962. The role of aluminum in igneous clinopyroxenes with relation to their parentage. *American Journal of Science.* 260 :267-288. DOI: https://doi.org/10.2475/ajs.260.4.267

Le Maître, R.W., 2005. *Igneous Rocks: A Classification and Glossary of Terms: Recommendations of the International Union of Geological Sciences Subcommission on the Systematics of Igneous Rocks*. 2nd Edition. Cambridge University Press. 256 p.

Longpré, M. A., Troll, R. V. & Hasteen, T. H. 2008. Upper mantle magma storage and transport under a Canarianshield-volcano, Teno, Tenerife (Spain). *Journal of Geophysical Research.* 113(B08) :203. DOI: https://doi.org/10.1029/2007JB005422

Marimoto, N. 1988. Nomenclature of Pyroxenes. *Mineralogy and Petrology.* 39(1) :55. DOI: https://doi.org/10.1007/BF01226262

Marques, L.S. *et al.* 1999. Petrology, geochemistry and Sr–Nd isotopes of the Trindade and Martin Vaz volcanic rocks (Southern Atlantic Ocean). *Journal of Volcanology and Geothermal Research*. 93(3-4) :191–216. DOI: http://doi.org/10.1016/S0377-0273(99)00111-0

McDonough, W.F. & Sun, S.-S. 1995. Composition of the Earth. *Chemical Geology*. 120 :223-253. DOI: https://doi.org/10.1016/0009-2541(94)00140-4

Mollo, S., & Vona, A. 2014. The geochemical evolution of clinopyroxene in the Roman Province: A window on decarbonation from wall-rocks to magma. *Lithos*. 192 :1-7. DOI: https://doi.org/10.1016/j.lithos.2014.01.009

Neave, D. A. & Putirka, K. D. 2017. A new clinopyroxene-liquid barometer, and implications for magma storage pressures under Icelandic rift zones. *American Mineralogist.* 102 (4) :777-794. DOI: https://doi.org/10.2138/am-2017-5968

Neumann, E.R., Wuff-Pedersen, E., Simonsen, S.L., Pearson, N.J., Marti, J. & Mitjavila, J. 1999: Evidence for fractional crystallization of periodically refilled magma chambers in Tenerife, Canary Islands. *Journal of Petrology*. 40 :1089-1123. DOI: https://doi.org/10.1093/petroj/40.7.1089

Pearce, T.H. & Kolisnik, A.M. 1990. Observation of plagioclase zoning using interference imaging. *Earth-Science Reviews.* 29(1-4) :9–26. DOI: https://doi.org/10.1016/0012-8252(0)90024-P

Putirka, K. 1999. Clinopyroxene + liquid equilibria to 100 kbar and 2450 K. *Contributions to Mineralogy and Petrology*, 135(2-3), 151-163.

Putirka, K. D., Perfit, M., Ryerson, F. J., & Jackson, M. G. 2007. Ambient and excess mantle temperatures, olivine thermometry, and active vs. passive upwelling. *Chemical Geology.* 241(3-4) :177-206. DOI: https://doi.org/10.1016/j.chemgeo.2007.01.014

Putirka, K. D. 2008. Thermometers and Barometers for Volcanic Systems. *Reviews in Mineralogy and Geochemistry.* 69 (1): 61-120. DOI: https://doi.org/10.2138/rmg.2008.69.3

Rhodes, J.M., Dungan, M.A., Blanchard, D.P. & Long, P.E., 1979. Magma mixing at mid-ocean ridges: evidence from basalts drilled near 22 N on the Mid-Atlantic Ridge. *Tectonophysics.* 55(1–2) :35–61. DOI: https://doi.org/10.1016/0040-1951(79)90334-2

Roeder, P.L. & Emslie, R.F. Olivine-liquid equilibrium. Contributions to Mineralogy and Petrology, v. 29(4), p. 275-289, 1970. Doi: https://doi.org/10.1007/BF00371276

Santos, Anderson Costa dos. 2016. *Petrology of Martin Vaz Island and Vitória-Trindade Ridge seamounts: Montague, Jaseur, Davis, Dogaressa and Columbia. Trace elements, 40Ar/39Ar dating and Sr and Nd isotope analysis related to the Trindade Plume evidences.* 218 f. Thesis (PhD in Geology) – Faculdade de Geologia, Universidade do Estado do Rio de Janeiro, Rio de Janeiro.

Santos, Anderson Costa dos. 2013. *Petrography, Lithogeochemistry and 40Ar/39Ar dating of the seamounts and Martin Vaz Islands - Vitoria-Trindade Ridge.* 115 f. Dissertation (M.Sc. Geology) - Faculty of Geology, University of Rio de Janeiro State, Rio de Janeiro.

Santos, A. C. Geraldes, M. C. Vargas, T. Willians, S., 2015. Geology of Martin Vaz. South Atlantic. *Journal of* Maps, 11(2): 314-322. DOI: https://doi.org/10.1080/17445647.2014.936913

Santos, A. C., Geraldes, M. C., Siebel, W., Mendes, J., Bongiolo, E., Santos, W. H., Garrido, T. C. V. & Rodrigues, S. W. O. 2018a. Pleistocene alkaline rocks of Martin Vaz volcano, South Atlantic: low-degree partial melts of a CO_2 - metasomatised mantle plume. *International Geology Review.* 61(3) :296-313. DOI: http://doi.org/10.1080/00206814.2018.1425921

Santos, R.N. & Marques, L.S. 2007. Investigation of 238U-230Th-226Ra and 232Th-228Ra-228Th radioactive disequilibria in volcanic rocks from Trindade and Martin Vaz Islands (Brazil; Southern Atlantic Ocean). *Journal of Volcanology and Geothermal Research.* 161 :215-233. DOI: https://doi.org/10.1016/j.jvolgeores.2006.11.010

Scorza, E. P. 1964. Duas Rochas Alcalinas das Ilhas Martin Vaz - Notas Preliminares e Estudos. *Departamento Nacional de Produção Mineral (DNPM). Divisão de Geologia e Mineralogia, Rio de Janeiro.* 121 :1-7.

Siebel. W. et al. 2000. Trindade and MartinVaz Island. South Atlantic: isotopic (Sr, Nd, Pb) and trace element constraints on plume related magmatism. *Journal of South American Earth Sciences*. 13(1) :79-103. DOI: http://dx.doi.org/10.1016/S0895-9811(00)00015-8

Takahashi, E., Uto, K., & Schilling, J. G. 1987. Primary magma compositions and Mg/Fe ratios of their mantle residues along Mid Atlantic Ridge 29 N to 73 N. *Technical Rept*. ISEI Ser. A, 9 :1-14.

Xu, Y. et al. 2003. Highly magnesian olivines and green-core clinopyroxenes in ultrapotassic lavas from western Yunnan, China: evidence for a complex hybrid origin. *European Journal of Mineralogy*. 15(6) :965-975. DOI: https://doi.org/10.1127/0935-1221/2003/0015-0965

Supplementary Material

Supplementary Table 1 – P-T clinopyroxene-liquid pair according to Dr. Keith Putirka excel spreadsheet. Details on thermobarometers models are inside the spreadsheet.

Supplementary Table 2 – Silica-activity barometer according to Dr. Keith Putirka excel spreadsheet. Whole rock model, temperatures estimates by clinopyroxene-liquid model was used in this table. Details on the model are inside the spreadsheet.

Supplementary Table 3 – Olivine-liquid thermometer for the Bandeira Unit samples, according to Dr. Keith Putirka excel spreadsheet. Details on the model are inside the spreadsheet.

Supplementary Table 4 – Petro Mode excel spreadsheet with modal calculation from whole rock composition and major element mass balance calculation to test the derivation of a daughter liquid from a parent liquid by removal of mineral phases.

HIGHIGHTS

- We detail new textural petrographic, mineral chemistry and geothermobarometric data of green-core clinopyroxenes from Martin Vaz Archipelago.
- Mineral chemistry indicates that Al-Ti-$^{Fe3+}$-Ca richer rims were generated after an input of primitive Ca-rich magma in the magmatic chamber.
- Resorbed olivines without melt-cpx-equilibrium probably related to hybrid origin.
- Geothermobarometric data suggest a polybaric evolutionary history.

[1a]André Leite de Oliveira; [1b]Anderson Costa dos Santos; [1c]Camila Cardoso Nogueira; [1d]Thaís Mothé Maia; [1e]Mauro César Geraldes

[1]Universidade do Estado do Rio de Janeiro (UERJ), Faculdade de Geologia, Departamento de Mineralogia e Petrologia Ígnea (DMPI). São Francisco Xavier Street, 524 - 4033A, Rio de Janeiro (RJ), Brazil, [1b*] Tektos and GeoAtlântico groups, Rio de Janeiro State University/Geobiotec, Geosciences Department, Aveiro University, 3810-193 Aveiro, Portugal.

Authors' Affiliations

1. André Leite de Oliveira: Universidade do Estado do Rio de Janeiro (UERJ), Faculdade de Geologia, Departamento de Mineralogia e Petrologia Ígnea (DMPI).
2. Anderson Costa dos Santos: Universidade do Estado do Rio de Janeiro (UERJ); Tektos Group (Universidade do Estado do Rio de Janeiro - UERJ); GeoAtlântico Group (Geobiotec, Geosciences Department, Aveiro University).
3. Camila Cardoso Nogueira: Universidade do Estado do Rio de Janeiro (UERJ), Faculdade de Geologia, Departamento de Mineralogia e Petrologia Ígnea (DMPI).
4. Thaís Mothé Maia: Universidade do Estado do Rio de Janeiro (UERJ), Faculdade de Geologia, Departamento de Mineralogia e Petrologia Ígnea (DMPI).
5. Mauro César Geraldes: Universidade do Estado do Rio de Janeiro (UERJ), Faculdade de Geologia, Departamento de Mineralogia e Petrologia Ígnea (DMPI).

Declaration of interests

☒ The authors declare that they have no known competing financial interests or personal relationships that could have appeared to influence the work reported in this paper.

☐The authors declare the following financial interests/personal relationships which may be considered as potential competing interests: